

A Dual Two Level PV Inverter without an Isolation Transformer

C. Ganesh¹, S. Sarada² and P. Bala Guravaiah³

Assistant Professor, Dept. EEE, A.I.T.S-Rajampet, A.P, India.

Assistant Professor, Dept. EEE, A.I.T.S-Rajampet, A.P, India.

P.G. Student, Dept. EEE, A.I.T.S-Rajampet, A.P, India.

Abstract

This paper examines the use of a dual bridge Inverter topology for an induction machine drive application. It considers the possibility of using a dual bridge inverter with one bridge floating to generate multilevel output voltage waveforms by solar PV cell with RippleCorrelationControl MPPT. The charging and discharging of the floating capacitor will be controlled using redundant switching states. The use of this topology can improve system efficiency and converter volume. The paper includes analysis and modulation of the converter topology as well as simulation and practical results showing the converter operation.

Keywords-Space vector, Open End Winding Induction Machine (OEWIM), Dual inverter, Floating Bridge (FB),and Main Bridge (MB).Ripple Correlation control

I. INTRODUCTION

This paper depicts a novel force converter topology for a three-stage engine with open finished windings. This machine topology is considered as it has a few focal points in engine drive applications where excess and adaptation to internal failure are worthwhile. The utilization of a double inverter span permits the converter to imitate the waveforms found in a three level NPC converter whilst disposing of the

requirement for capacitor adjusting procedures. The benefits of double extension inverter as for single finished inverters include:

- Improved accessibility since adaptation to non-critical failure can be presented.
- Reduced voltage blocking prerequisites for a portion of the force semiconductors
- Inverters can share changing occasions prompting lower singular gadget compensation frequencies.
- Reduced exchanging misfortunes for a given yield waveform quality

Double inverter topologies have been considered in various papers for various applications. Customary double inverter topologies (utilizing two disconnected dc sources) are investigated. In these papers, distinctive space vector adjustment plans have been utilized to create multilevel yield voltage waveforms. A square chart of a customary Open End Winding Induction Motor (OEWIM) drive is exhibited in Fig.1. It is conceivable to utilization of a solitary supply for double inverters with a typical mode disposal system. These topologies use particular exchanging mixes that produce measure up to regular mode voltages which cross out at burden terminals.

Decrease in voltage levels and lower dc transport usages are the primary hindrances of this kind of topology. An adjustment method to adjust power between the two inverters in a double inverter framework has likewise been proposed. This topology still uses a disengagement transformer; the extent of this transformer can be diminished to the detriment of decreased adjustment file. The skimming capacitor span topology is introduced in alongside a control plan to permit supply of receptive force. Different creators have exhibited a technique to make up for supply voltage hang with a specific end goal to keep the drive operational amid steady power mode.

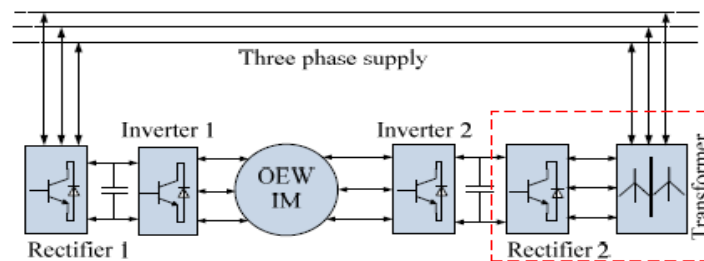


Fig.1: Conventional open end winding IM drive topology

This topology additionally utilizes a gliding capacitor extension to counterbalance the voltage hang in fast machines. To evacuate the segregation transformer and accomplish multilevel yield voltage waveforms, a double inverter with a drifting capacitor scaffold is considered. This paper likewise shows a balance plan which just uses changing state redundancies to charge and release the skimming span capacitor. The proposed balance system does not require request reference voltage era to charge

the coasting capacitor, in this manner killing the danger of making undesirable sounds in the yield voltage waveforms.

II. PROPOSED SYSTEM

A. Floating capacitor bridge inverter

The coasting span capacitor double inverter based topology has beforehand been broke down for various applications. The circuit can be utilized to supply receptive energy to a machine and to adjust for any supply voltage hang. In both cases the likelihood of multilevel yield voltage waveforms were not considered. In this paper the capacitors in the gliding inverter scaffold is charged utilizing repetitive changing mixes to evacuate the confinement transformer and to accomplish multilevel yield voltages. Fig. 2 demonstrates the piece graph of the double inverter with a skimming span capacitor. Sources utilized here depend on a proportion of 2:1. The utilization of this specific proportion licenses double two level inverters to create up-to a four level yield shaft voltage waveform.

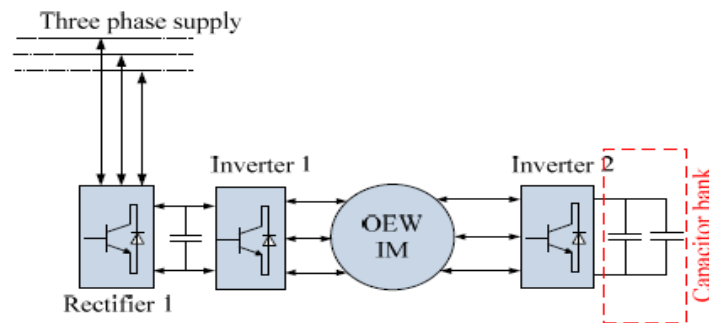


Fig.2: Block diagram of proposed floating bridge topology

B. Principles of operation

To show how the capacitor can be charged and discharged the switching combinations can be analysed. The dual inverter topology, shown in Fig. 3, is considered assuming that each inverter is fed from isolated sources. The space vector diagram for the converter modulations is shown in Fig.4.

In Fig.4, the red numbered switching combinations discharges the floating bridge capacitor, while the green numbered switching combinations charge the capacitor and the yellow numbered switching combinations hold the last state of capacitor.

To assess how these combinations will charge or discharge the floating capacitor, the current flow for different switching combinations are examined. To make the analysis brief only one half of the sector is taken into consideration, the red triangle as shown in Fig. 4. The other half of the triangle is a mirrored image and this is then repeated around the state diagram.

S3) of the two level inverter legs, where '+' refers to the on state and '-' refers to the off state of power semiconductor switching devices. Numbers with a superscript (') denotes the switching state combination for second, lower voltage, inverter. It can be seen from the Fig. 5 that combinations (11') and (16') will result in a current through the capacitor from the positive to the negative terminal, thus charging the capacitor. Combinations (14'), (15') and (74') will result in a current in the other direction and will therefore act to discharge the capacitor. Combinations ending with 7 (111) or 8 (000) will hold the capacitor's charge at its previous state. It is evident from the state diagram that if the reference voltage resides in outer hexagon then there are only two switching combinations in each sector to charge the floating capacitor. This is insufficient to maintain the charge under all operating conditions; therefore a restriction has to be imposed. As a result the achievable voltage level is reduced (voltage levels being equal to three level NPC converters) along with lower than ideal DC bus utilization. The capacitor can charge to half of the main DC link only if the modulation index (m) is limited as shown in equation 1.

$$0 < m \leq 0.6 \tag{1}$$

Violation of the imposed restriction will cause the capacitor voltage to collapse.

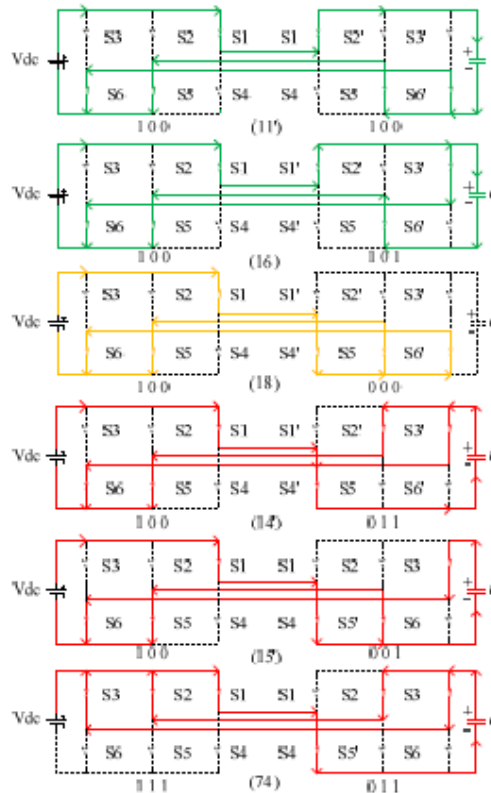


Fig.5: The current flow for different switching state combinations.

C. Modulation strategy

A decoupled space vector modulation strategy can be adopted for this dual inverter floating bridge capacitor topology. Switching combinations are selected in such a way that generated voltages for each of the converters that are 180 degree phase shifted from the other, as shown in Fig. 6. The voltages will add at the load terminal to match the overall reference. The combined reference voltage will be located in sector 1 (subsector 7), which is shown in Fig. 7.

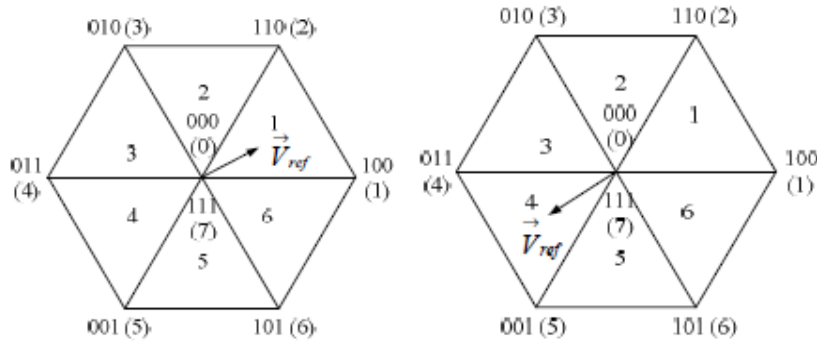


Fig.6: Space vector diagram of individual inverters

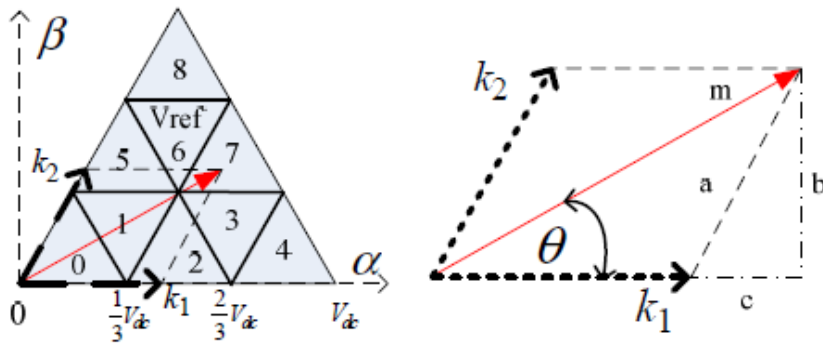


Fig.7: Sub sector identification

$$a=k_2 = \frac{b}{\sin(\frac{\pi}{3})} = \frac{2}{\sqrt{3}}b = \frac{2}{\sqrt{3}}m\sin(\theta) \tag{2}$$

$$k_1=m\cos(\theta) - \left(\frac{2}{\sqrt{3}}m\sin(\theta)\right)\cos(\frac{\pi}{3})$$

$$k_1=m\left(\cos(\theta) - \frac{\sin(\theta)}{\sqrt{3}}\right) \tag{3}$$

$$m = \frac{\sqrt{3}V_{ref}}{V_{dc}} \tag{4}$$

The switching sectors for the dual inverter are identified using angle of the reference voltage. Each sector is 60 degree apart from the adjacent one. First the angle of the reference voltage is identified and then using a simple ‘else – if’ statement is used to identify the sectors. The process of identifying reference voltage subsector location is shown in equations 2 to 4 and Table I.

TABLE-I: Subsector Identification

Subsector	Identification criteria
0	$if ((k_1, k_2) < \frac{1}{3} \ \& \ (k_1 + k_2) \leq \frac{1}{3})$
1	$if ((k_1, k_2) < \frac{1}{3} \ \& \ (k_1 + k_2) > \frac{1}{3})$
2	$if (k_1 < \frac{2}{3} \ \& \ k_2 < \frac{1}{3} \ \& \ (k_1 + k_2) < \frac{2}{3})$
3	$if (k_1 < \frac{2}{3} \ \& \ k_2 < \frac{1}{3} \ \& \ (k_1 + k_2) > \frac{2}{3})$
4	$if (k_1 > \frac{2}{3})$
5	$if (k_1 < \frac{1}{3} \ \& \ k_2 > \frac{1}{3} \ \& \ (k_1 + k_2) < \frac{2}{3})$
6	$if (k_2 < \frac{2}{3} \ \& \ k_1 < \frac{1}{3} \ \& \ (k_1 + k_2) > \frac{2}{3})$
7	$if (k_2 < \frac{2}{3} \ \& \ k_1 < \frac{2}{3} \ \& \ (k_1 + k_2) > \frac{2}{3})$
8	$if (k_2 > \frac{2}{3})$

The equations are derived using Fig. 7. The switching time is calculated using the volt second balancing principle. An example of how to calculate the timings when reference voltage resides on sector 1 (subsector 1) is presented in equations 5 and 6.

$$V_{ref}T_1(\cos(\theta) - j\sin(\theta)) = V_1T_1 + V_2T_2 + V_3T_3 \tag{5}$$

Where

$$V_1 = \frac{2}{9} V_{dc} e^{j0} \tag{6}$$

$$V_2 = \frac{2}{9} V_{dc} e^{j60}$$

$$V_3 = \frac{2}{3\sqrt{3}} V_{dc} e^{j30}$$

Equations are then manipulated to find T_1, T_2 & T_3

Finally, a seven segment switching sequence is used to modulate the reference voltage as shown in Fig. 8. In Fig. 8 a superscript refers to the floating inverter legs. Switching combinations are selected in such a way that when floating capacitor voltage is lower than demand reference voltage the charging combinations will be selected and it will choose all the discharging combinations when capacitor voltage is higher than the reference voltage. Table II presents the charging and discharging switching combinations when reference voltage resides in sector 1 of the vector diagram. As the outer hexagon is not used switching sequences for outer hexagon are not presented in this paper.

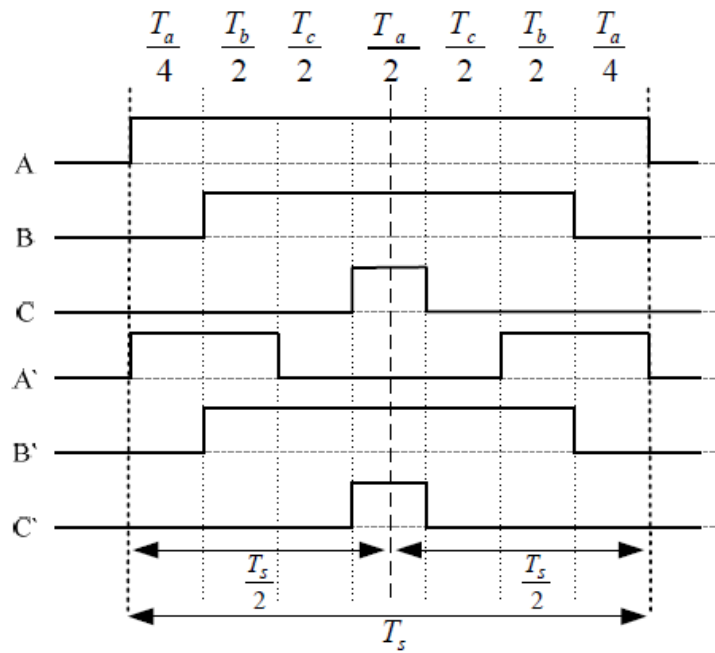


Fig.8: Seven segment switching sequence (sector 1, subsector 1)

TABLE-II: Switching Combinations

Sub sector	Charging				Discharging			
	T _a	T _b	T _c	T _a	T _a	T _b	T _c	T _a
0	88	11	22	77	87	84	85	88
1	11	22	23	74	84	85	16	74
2	11	16	17	84	84	16	17	84
5	22	23	27	85	85	23	27	22

III. PHOTOVOLTAIC (PV) CELL WITH RCC MPPT

In proposed method is used in the three phase supply and replace by using solar Photovoltaic (PV) cell with RCC MPPT Algorithm method is used.

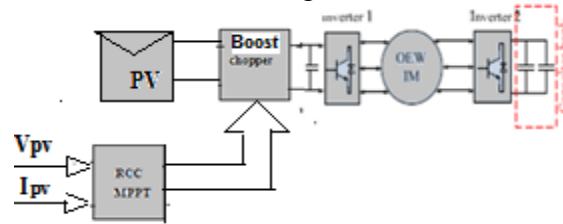


Fig 9: Block diagram of PV cell with RCC MPPT

Ripple correlation control (RCC) was first proposed by Midyaet *al.* (1996) for MPPT and motor efficiency optimization purposes. Inexpensive and robust controllers utilizing an analog RCC technique have also been developed by Esramet *al.* (2007), Il-Song & Myung-Joong (2004) and Lim & Hamill (2000, 2001). RCC makes use of converter ripple as an alternate source of perturbation. The maximum power point is usually located by correlating the derivative of the array power with the voltage or current ripple waveform. As Midyaet *al.* (1996:1710) note, a major benefit of RCC is that it ‘keeps [DC–DC] converter operation at the optimum point’ while avoiding the ‘inconvenient, slow, and fundamentally sub-optimal’ perturbation process described in previous sections.

The concept of distributed generation has enabled any individual single-phase consumer to generate power and also sell the excess power to the utility grid. Because of this, small single phase photovoltaic (PV) generating units are becoming more and more popular. Such distributed units should be operated reliably without much maintenance and should be cost effective.

A typical single phase grid connected PV system has more than one stage of energy conversion. The first stage is usually a dc-dc converter, which boosts the dc-link voltage level such that it can draw peak available power from PV panels. The second stage is an inverter, which ensures that whatever the energy extracted from PV array is fed to the utility grid.

The cost and complexity of the system can be reduced by employing a single-stage topology. Moreover, such a system can be more reliable, because of the reduced component count.

As the average value of error signal indicates the distance of the operating point from MPP, the operating point can be controlled by passing the average error signal through a PI controller. The implementation of the proposed MPPT algorithm is shown in Fig.11. The ripples $\tilde{v}(t)$ and $\tilde{p}(t)$ can be obtained by subtracting the average values from the respective signals using LPFs. The product of these ripples is used as input to a PI controller. The output of the PI controller is considered as reference signal, $V^*(t)$ to control the dc-link voltage.

The reference signal thus obtained is compared with PV array voltage and the error obtained is passed through another PI controller to obtain the load angle δ . This angle is used to generate the control signals to operate the inverter switches.

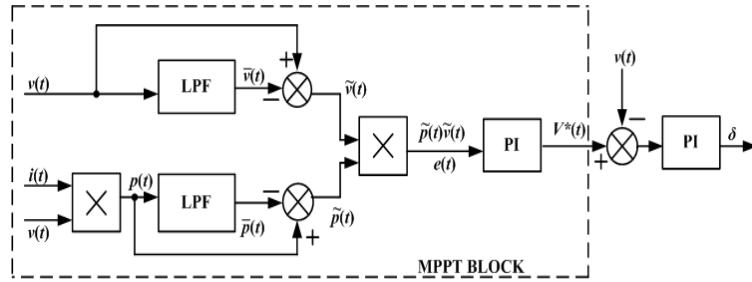


Fig. 11: Block diagram showing implementation of the proposed MPPT algorithm.

IV.SIMULATION RESULTS

The proposed modulation scheme has been simulated using MATLAB and PLECS. Fig. 12 shows the charging and discharging of floating SSS capacitor voltage. To obtain a multilevel inverter topology main bridge inverter is supplied with 260 V dc and then the floating capacitor is charged to 130 V. The system is connected to an open phase R-L load. Parameters of the load and induction machine are presented in Table

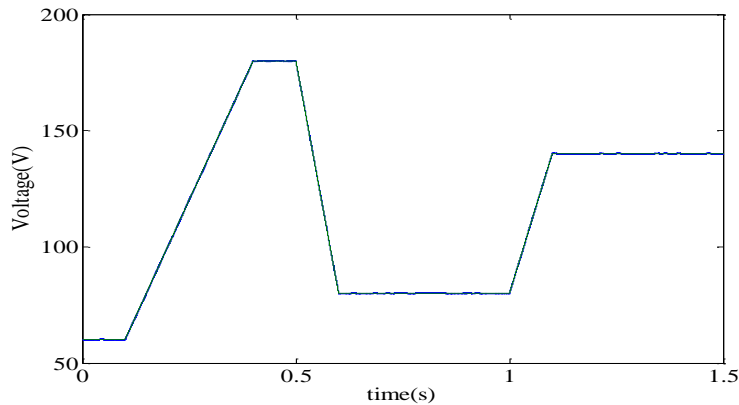


Fig.12: Charging and discharging of capacitor

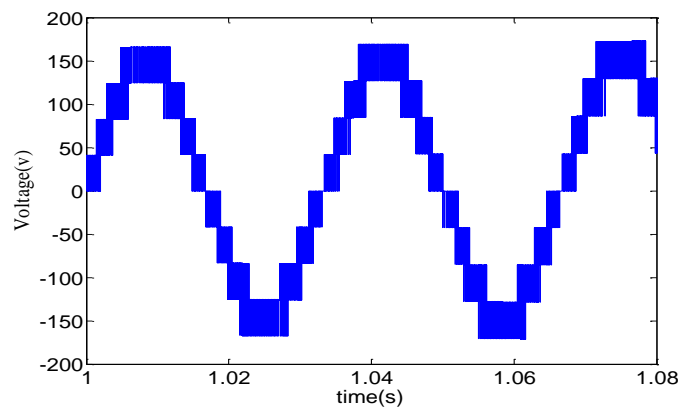


Fig.13: Phase voltage (Phase A - measured across AA' Fig. 3)

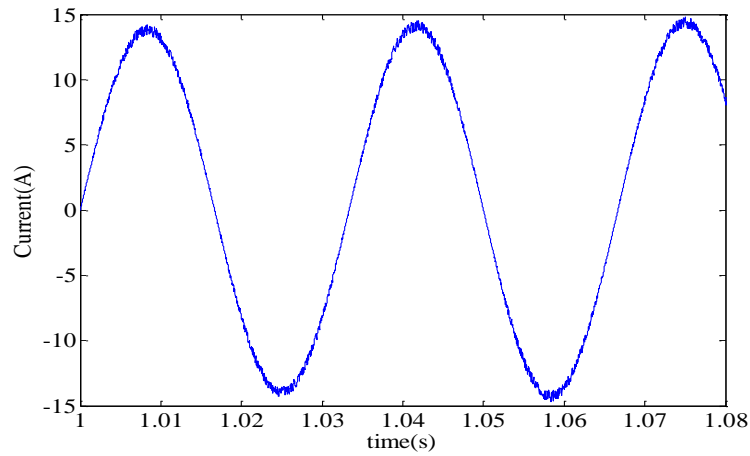


Fig.14: Phase current (Phase A)

TABLE III: Load Parameters

R-L LOAD		
Resistance	R	10 Ohm
Inductance	L	3.75e-3H
INDUCTION MOTOR		
Stator resistance	R_s	1.4 Ohm
Rotor resistance	R_r	1.23 Ohm
Stator leakage inductance	L_{ls}	0.0115H
Rotor leakage inductance	L_{lr}	0.009258H
Magnetizing inductance	L_m	0.2258H

A voltage of 30 Hz and 135 V is demanded from the dual inverter at a modulation index of 0.6. The output voltage and currents are shown in Fig 12 and Fig 13. It can be seen from the simulation results that the floating bridge capacitor is charged to the required value and the dual inverter system can achieve a multilevel output voltage waveform.

CONCLUSION

A motor drive using an open ended winding machine and a dual bridge inverter topology with a solar floating Capacitor Bridge has been analysed and demonstrated.

The proposed system charges the floating bridge capacitor to a ratio of 2:1 with respect to main bridge DC link voltage amplitude. This particular DC link voltage ratio allows the converter to achieve multi-level output voltage waveform. The floating DC link voltage is kept at a constant voltage by the means of charging and discharging the floating bridge capacitor. This is achieved by deploying a slow controller to switch between charging and discharging redundant states of the converter. The proposed system has been simulated to validate the results. It has been shown that the proposed system can charge the capacitor to the required voltage and can achieve a multilevel output voltage waveform.

REFERENCES

- [1] Ertugrul, N., et al. Fault tolerant motor drive system with redundancy for critical applications. in Power Electronics Specialists Conference, 2002.pesc 02. 2002 IEEE 33rd Annual. 2002.
- [2] Ahmed, S.M.W., et al. Open ends induction motor operation based on a dual inverter. in Design and Test Workshop (IDT), 2009 4thInternational. 2009.
- [3] Ahmed, S.M.W., G.M.A. Sowilam, and A.b.S.M. Salim. Practical implementation of a dual inverter operates open ends induction motor. In Design and Test Workshop (IDT), 2009 4th International. 2009.
- [4] Rama Chandra sekhar, K., S. Mohan, and S. Srinivas. An improved PWM for a dual two-level inverter fed open-end winding induction motor drive. in Electrical Machines (ICEM), 2010 XIX International Conference on. 2010.
- [5] Shiva kumar, E.G., et al. Space vector PWM control of dual inverter fed open-end winding induction motor drive. in Applied Power Electronics Conference and Exposition, 2001. APEC 2001.Sixteenth Annual IEEE.2001.
- [6] Soma sekhar, V.T., et al. A novel PWM inverter switching strategy for a dual two-level inverter fed open-end winding induction motor drive. In Power Electronics and Drive Systems, 2001.Proceedings., 2001 4thIEEE International Conference on. 2001.
- [7] Zhao, Y. and T.A. Lipo, Space vector PWM control of dual three-phase induction machine using vector space decomposition. Industry Applications, IEEE Transactions on, 1995. 31(5): p. 1100-1109.
- [8] Baiju, M.R., et al., A dual two-level inverter scheme with common mode voltage elimination for an induction motor drive. Power Electronics, IEEE Transactions on, 2004. 19(3): p. 794-805.
- [9] Kalaiselvi, J., K.R.C. Sekhar, and S. Srinivas. Common mode voltage elimination PWMs for a dual two-level VSI with single inverter switching. in Industrial Electronics (ISIE), 2012 IEEE International Symposium on. 2012.

- [10] Grandi, G. and D. Ostojsic. Dual inverter space vector modulation with power balancing capability.in EUROCON 2009, EUROCON '09. IEEE.2009.
- [11] Grandi, G., et al. Multilevel Operation of a Dual Two-Level Inverter with Power Balancing Capability. in Industry Applications Conference,2006. 41st IAS Annual Meeting.Conference Record of the 2006 IEEE.2006.
- [12] Ewanchuk, J. and J. Salmon. A Square-wave Controller for a high speed induction motor drive using a three phase floating bridge inverter.In Energy Conversion Congress and Exposition (ECCE), 2010 IEEE. 2010.
- [13] Haque, R.U., et al. PWM control of a dual inverter drive using an open-ended winding induction motor. in Applied Power Electronics Conference and Exposition (APEC), 2013 Twenty-Eighth Annual IEEE.2013.
- [14] Ewanchuk, J., J. Salmon, and C. Chapelsky, A Method for Supply Voltage Boosting in an Open-Ended Induction Machine Using a Dual Inverter System With a Floating Capacitor Bridge. Power Electronics,IEEE Transactions on, 2013. 28(3): p. 1348-1357

